Research Paper

A hybrid design to optimize preparation of lopinavir loaded solid lipid nanoparticles and comparative pharmacokinetic evaluation with marketed lopinavir/ritonavir coformulation

Punna Rao Ravi, Rahul Vats, Vikas Dalal and Aditya Narasimha Murthy

Pharmacy Department, BITS-Pilani Hyderabad Campus, Hyderabad, Andhra Pradesh, India

Abstract

Objectives To prepare stearic acid-based lopinavir (LPV) loaded solid lipid nanoparticles (SLNs) using a hybrid design and compare in-vivo performance of optimized formulation with marketed LPV/ritonavir (RTV) coformulation.

Methods LPV SLNs were prepared by hot melt emulsion technique and optimized using Plackett–Burman design and Box–Behnken design. Physical characterization studies were conducted for the optimized SLNs. Comparative oral pharmacokinetic studies and tissue distribution studies of optimized SLNs and LPV/RTV coformulation were done in Wistar rats. In-vitro metabolic stability and intestinal permeability studies for LPV SLNs were undertaken to elucidate the mechanism involved in the pharmacokinetic improvement of LPV.

Key findings Optimized SLNs exhibited nanometeric size (223 nm) with high entrapment efficiency (83%). In-vitro drug release study of SLNs showed biphasic sustained release behaviour. Significant increase in oral bioavailability of LPV from LPV SLNs (5 folds) and LPV/RTV coformulation (3.7 folds) was observed as compared with free LPV. LPV SLNs showed better tissue distribution of LPV in HIV reservoirs than LPV/RTV coformulation. In-vitro studies demonstrated that SLNs provided metabolic protection of LPV and were endocytosized during absorption.

Conclusions SLNs enhanced oral bioavailability and improved distribution profile of LPV to HIV reservoirs and hence could be better alternative to LPV/RTV coformulation.

Introduction

AIDS is a disease of human immune system caused by HIV. This condition progressively reduces effectiveness of immune system and leaves individuals susceptible to opportunistic infections and tumors.[1] In the human body, HIV mainly resides in anatomical (central nervous system, lymphatic system, liver, lungs and the genitals) and cellular reservoirs (i.e. CD+ T lymphocytes and monocytes/macrophages).[2] However, majority of antiretroviral drugs are unable to reach these 'viral reservoirs'/HIV localization sites due to poor organ perfusion and surface permeability glycoprotein (P-gp) efflux.[3] HIV remains viable in these viral reservoirs even when sufficient concentration of drug is available in blood.[4,5]

Lopinavir (LPV) is a newer and more promising HIV protease inhibitor. It is an essential part of highly active antiretroviral therapy and a new standard of care for HIV-infected patients in antiretroviral therapy.[6] LPV shows poor oral bioavailability as it is substrate for both cytochrome P450 3A4 (CYP3A4) and P-gp systems present in liver and intestine.[7,8] When given alone, LPV fails to achieve therapeutic concentration in blood and viral reservoirs as it is susceptible to extensive firstpass metabolism.[9]

In order to improve oral bioavailability of LPV, ritonavir (RTV) is coformulated with LPV at subtherapeutic dose levels as a booster regimen (Kaletra, Abbott laboratories, North Chicago, IL, USA).[10] RTV has been reported to enhance oral bioavailability of LPV because of its inhibitory action on CYP3A4 and P-gp.[11] However, RTV used in this combination could cause glucose intolerance, gastrointestinal intolerance, lipid elevations and perioral parasthesia.[12]

Thus, there is a need of RTV-free strategy to improve LPV's oral bioavailability and to achieve optimum LPV concentration in HIV localization sites.

In recent times, solid lipid nanoparticles (SLNs) have shown potential as effective drug carriers to target lymphatic system.[13] The nanometric size of these carriers allows for efficient crossing of biological barriers, improves cellular uptake and drug exposure by avoiding first pass metabolism, P-gp-mediated efflux and promoting intestinal lymphatic transport.[14]

Use of SLNs in targeting lymphatic system and improving oral bioavailability of LPV has been recently reported.[15,16] These studies show a significant increase in plasma exposure of LPV when loaded in SLNs. However, for pragmatic purposes, more logical approach in development of SLN formulation is needed. US FDA suggests use of Quality by Design approach to develop any formulation, of which, design of experiments (DoE) is an integral part.[17] In this study, for the first time, we have compared in-vivo performance of optimized SLN formulation with marketed formulation, which makes it more clinically relevant. We optimized LPV SLNs using stearic acid (SA) as a model lipid. SA was chosen due to its biodegradability, biocompatibility and for economic reasons.[18]

Primary objective of present work was to prepare and characterize LPV-loaded SLNs and to compare in-vivo performance of optimized formulation with marketed LPV/RTV coformulation. For optimization of LPV SLNs, DoE was used. Plackett–Burman design (PBD) and Box–Behnken design (BBD) were employed in sequence for rational design of LPV SLNs, and data were statistically analyzed using Design Expert software (Full version 8.0.7.1, Stat-Ease Inc., Minneapolis, MN, USA).

Materials and Methods

Materials

LPV and RTV were obtained as a gift sample from Matrix Laboratories, Hyderabad, India. Lopimune tablet (LPV/RTV coformulation; 200/50 mg; Cipla Ltd., Mumbai, India) was purchased locally form Indian market. SA and polyvinyl alcohol (PVA) were purchased from Sigma-Aldrich, Mumbai, India. Rat intestinal microsomes (RIM), rat liver microsomes (RLM) and nicotinamide adenine dinucleotide phosphate (NADPH) were procured from BD Gentest (Woburn, MA, USA). HPLC grade acetonitrile, ammonium acetate, methanol and sodium citrate were purchased from Merck Laboratories, Mumbai, India. Ingredients of Krebs–Henseleit bicarbonate (KHB) buffer were purchased individually from Sigma-Aldrich. Methyl cellulose (MC) and Tween 80 were purchased from S.D. Fine Chemicals Ltd, Mumbai, India. A Milli-Q water purification system

(Millipore, MA, USA) was used for obtaining high-quality HPLC grade water.

Methods

Preparation of solid lipid nanoparticles

LPV SLNs were prepared by previously reported warm oil-in-water microemulsion dispersion technique.[19] Briefly, SA (quantity varied as per experimental design) was held in a molten state at 75°C and accurately weighed quantity of LPV (20 mg) was dispersed thoroughly in it to form homogenous dispersion. Aqueous phase (25 ml) was prepared by dissolving PVA (quantity varied as per experimental design) into high-purity water, which was then heated. When temperatures of both the phases became isothermal, hot surfactant solution was added to molten lipid phase under homogenization (Polytron PT 3100D, Kinematica, Switzerland) at 10 000 rpm for 3 min while maintaining the temperature at 75 ± 0.5°C. The obtained microemulsion was quickly ultrasonicated using a probe sonicator (Vibra cell, Sonics, Newtown, CT, USA) for a specific time period at a constant amplitude (80 W output). The obtained o/w nanoemulsion was then cooled down in an ice-bath to form SLNs, and the volume was finally adjusted to 75 ml with high-purity cold water. This SLN dispersion in water was freeze-dried in a lyophilizer (Coolsafe 110–4, Scanvac, Denmark) with 5% w/v mannitol as a cryoprotectant for 12 h to obtain a free-flowing powder. The lyophilized powder was stored in air-tight glass containers at room temperature till further use.

Experimental design

The method for preparation of LPV SLNs involves several variables. To screen critical variables that affect quality attributes of SLN, a low resolution PBD was used. A total of 11 variables were studied at two levels to determine their influence on two responses, namely, entrapment efficiency percentage (EE %) and particle size of loaded SLN formulations. The variables studied were: type of surfactant (PVA and Tween 80), concentration of surfactant (0.5 and 1.5% w/v), temperature of surfactant solution (25 and 75°C), volume of external phase (10 and 30 ml), speed of homogenization (7500 and 12500 rpm), time of homogenization (2 and 8 min), amount of lipid (400 and 1200 mg), time of ultrasonication (5 and 15 min), amplitude of ultrasonication (70 and 100%), ultrasonication pulse (continuous and pulse mode) and temperature during homogenization (25 and 75°C).

Based on the results obtained from PBD, three critical variables that significantly affect EE and particle size were identified. These variables were further optimized using

Table 1 Variables and their levels in Box–Behnken design

Factor	Levels used		
	Low (–1)	Medium (0)	High (+1)
Independent variables			
X_1 = Surfactant concentration (% w/v)	0.5	1	1.5
X_2 = Lipid amount (mg)	400	800	1200
X_3 = Ultrasonication time (min)	5	10	15
Dependent variables	Constraints		
Y_1 = Particle size (nm)	Minimum		
Y_2 = Entrapment efficiency (%)	Maximize		

BBD. BBD, a subtype of response surface methodology, was employed to develop quadratic models for optimization process and to reduce the number of experimental trials. A 17-run, three-factor, three-level BBD was constructed to evaluate main effects, interaction effects and quadratic effects of identified initial factors. Nonlinear quadratic model generated by BBD design was in the following form Equation (1):

$$Y = b_0 + b_1 X_1 + b_2 X_2 + b_3 X_3 + b_{12} X_1 X_2 + b_{13} X_1 X_3 \\ + b_{23} X_2 X_3 + b_{11} X_1{}^2 + b_{22} X_2{}^2 + \boldsymbol{b}_{33} X_3{}^2 \qquad (1)$$

where, Y is measured response associated with each factor level combination; $b_0 - b_{33}$ are regression coefficients of respective factors, and their interaction terms computed from the observed experimental values of Y and X_1, X_2, X_3 are the coded levels of independent variables. The terms $X_1 X_2$, $X_2 X_3$, $X_3 X_1$ and $X_i{}^2$ ($i = 1$, 2 or 3) represent the interaction and quadratic terms, respectively. Dependent and independent variables selected are shown in Table 1. Critical variables evaluated in present study were surfactant concentration (X_1), lipid amount (X_2) and ultrasonication time (X_3). Responses studied were particle size (Y_1) and EE (Y_2). Experiment design matrix generated by software is presented in Table 2.

Particle size and zeta potential analysis

Particle size and zeta potential of prepared SLNs were measured by Zetasizer NanoZS (Malvern Instruments Ltd., Worcestershire, UK). All samples were suitably diluted with double distilled water prior to the measurement.

Entrapment efficiency determination

Drug EE was determined by previously published ultrafiltration method[20] with slight modification using microfilters (Amicon Ultra, Millipore, MA, USA; molecular weight cut-off (MWCO), 10 KDa). Briefly, microfilters containing 0.5 ml of SLNs suspended in water were centrifuged

at $6000 \times g$ for 30 min to separate un-entrapped drug (free drug, W_{free}) from total drug (W_{total}) added to the formulation. Un-entrapped drug (i.e. drug diffused through the membrane) was quantified by reverse phase liquid chromatographic (RP-HPLC) method. EE was calculated by following Equation (2):

$$EE\,(\%) = ((W_{total} - W_{free})/W_{total}) \times 100 \qquad (2)$$

Scanning electron microscopy analysis

Surface morphology of optimized SLN formulation was examined under scanning electron microscope (JSM-6360LV Scanning Microscope; Jeol, Tokyo, Japan). Before analysis, 100 µl of SLN dispersion was placed on an aluminum stub and dried overnight under vacuum. This was then sputter-coated using a thin gold-palladium layer under an argon atmosphere using a gold sputter module in a high-vacuum evaporator (JFC-1100 fine coat ion sputter; Jeol, Tokyo, Japan). These coated samples were then scanned and photomicrographs were taken at an acceleration voltage of 15 kV.

Differential scanning calorimetry

Differential scanning calorimetry (DSC) analysis was carried out using DSC 60 (Shimadzu, Kyoto, Japan) instrument. Accurately weighted samples were taken in an aluminium pan and crimp sealed. Samples were equilibrated at 25°C in DSC chamber. After sufficient equilibration time, samples were heated over a temperature range of 25 to 250°C with constant heating rate of 5°C/min during analysis.

In-vitro release study

Previously reported dialysis bag method[21] was used for in-vitro drug release study. Both free drug and LPV-loaded SLNs were studied for in-vitro release behaviour. For the study, a sealed dialysis bag (MWCO, 12–14 kDa, pore size 2.4 nm), containing free drug or SLNs equivalent to 1.5 mg LPV was completely submerged in 50 ml releasing media (PBS containing 0.1% w/v Tween 80, pH 7.4). Temperature of the media was maintained at $37 \pm 0.5°C$ and media was stirred at 50 rpm using magnetic bead. Drug release media was completely replaced at predetermined time intervals to maintain sink condition. Cumulative release of LPV in sample solution was determined by RP-HPLC method.

Obtained data were fitted into zero-order, first-order, Higuchi and reciprocal-powered time mathematical models for evaluation of release kinetics. Regression coefficient (r^2) and time for 50% dissolution (t_{50}) were calculated for the best-fit model.

Table 2 Box–Behnken experimental design

Run	Surfactant concentration (X_1, % w/v)	Lipid amount (X_2, mg)	Ultrasonication time (X_3, min)	Particle size (Y_1, nm)	Entrapment efficiency (Y_2, %)
1	1	800	10	218.5	83.0
2	0.5	800	15	367.8	59.8
3	0.5	800	5	372.5	59.2
4	1.5	400	10	299.0	62.0
5	1	400	15	366.8	51.8
6	1	800	10	220.0	77.0
7	1.5	800	5	327.8	75.8
8	0.5	1200	10	415.0	76.2
9	1	1200	5	309.5	80.0
10	1	400	5	239.3	55.0
11	0.5	400	10	353.4	45.1
12	1.5	1200	10	364.2	78.9
13	1	800	10	222.0	81.0
14	1.5	800	15	335.9	62.2
15	1	1200	15	316.2	71.7
16	1	800	10	217.0	77.4
17	1	800	10	221.0	81.1

Stability studies

Optimized SLN suspension was subjected to stability testing as per International Conference on Harmonization (ICH) Q1A (R2) guidelines.[22] Optimized LPV SLN suspension was stored in sealed glass vials at $25 \pm 2°C/60 \pm 5\%$ relative humidity in stability chamber (Remi, Mumbai, India). Control samples were stored at 2–8°C in a refrigerator. Both of these samples were analyzed at monthly intervals over a period of three months for particle size, zeta potential, polydispersity index (PDI) and EE. Statistical evaluation of observed data was done using GraphPad Prism version 5.03 for Windows software (GraphPad Software, San Diego, CA, USA).

Pharmacokinetic evaluation of optimized solid lipid nanoparticles in Wistar rats

Pharmacokinetic studies were performed using Male Wistar rats, weighing 180–220 g. Experimental protocol was approved by the Institutional Animal Ethics Committee (Approval No.: IAEC-01/01–12). All animals were housed under constant environmental conditions ($22 \pm 1°C$ room temperature; $55 \pm 10\%$ relative humidity; 12 h light/dark cycle) and were allowed access to food and water *ad libitum*. Animals were fasted overnight 12 h before dosing and continued on fasting until 4 h post administration of the formulation. Thereafter, rat chow diet was provided *ad libitum*. In all pharmacokinetic studies, LPV/RTV coformulation was prepared by crushing Lopimune tablets (Cipla Limited, Mumbai India; 200 mg/50 mg) and suspending in 0.5% w/v MC.

Based on study design, three different treatment groups were taken with five animals in each treatment group. Treatment groups were designated as: Group A (control group) – treated with LPV alone (20 mg/kg, LPV suspended in 0.5% w/v MC); Group B – treated with LPV/RTV coformulation (20/5 mg/kg); Group C- treated with optimized LPV SLN formulation (20 mg/kg).

Blood samples (150 μl) were withdrawn from rat orbital sinus and collected into microfuge tubes containing anticoagulant (3.8% w/v sodium citrate). Post-dosing, samples were collected at following time points: 0.17, 0.25, 0.5, 1, 2, 3, 4, 6, 8 and 12 h. These samples were further harvested for plasma by centrifuging at 4°C for 10 min at 650*g* and then stored at −70°C until further analysis. A validated HPLC method, previously reported[23] from our lab for estimation of LPV in rat plasma matrix, was used to analyze the samples.

Tissue distribution study

LPV biodistribution was assessed in male Wistar rats (180 ± 20 g; $n = 36$). The rats were randomly divided into three groups with 12 animals in each group. The groups were designated as: Group A (control group) – treated with LPV (20 mg/kg, LPV suspended in 0.5% w/v MC) alone; Group B – treated with LPV/RTV coformulation (20/5 mg/kg); Group C – treated with optimized LPV SLN formulation (20 mg/kg). Three rats from each group were sacrificed at 0.5, 1, 2 and 4 h post-dosing. Individual animals were perfused with heparinized (5 IU) saline (0.9% w/v NaCl) through the portal vein in order to remove circulating blood from body organs before tissue collection. Tissues of interest (liver, spleen and mesenteric lymph nodes) were collected and stored at −70°C until further analysis.

Prior to analysis, tissue samples were thawed to room temperature and minced. Using tissue homogenizer (Remi),

tissue samples were ground to a fine paste (25% w/v) with water : methanol mixture (4 : 1). LPV was extracted from tissue homogenate by adding acetonitrile in the ratio of 1 : 3 (v/v). Extracted samples were centrifuged (6000 × g for 15 min) and resultant clean supernatant (75 µl) was injected into HPLC to determine LPV concentration in tissue samples.

In-vitro metabolic stability study

In-vitro metabolic stability studies were performed by incubating free LPV, LPV/RTV (RTV at an effective concentration of 1.25 µM) coformulation and LPV SLNs with RIM and RLM (1 mg/ml) at an effective concentration of 5 µM. Reaction was initiated by addition of NADPH (2 mM) in phosphate buffer (100 mM, pH 7.4). Incubations were performed at 37°C in a shaking water bath for 30 min. Reaction was terminated by addition of cold acetonitrile. Samples were vortexed briefly and centrifuged at 6000*g* for 15 min. Resultant clean supernatant (75 µl) was injected in to HPLC. Percentage metabolism of LPV was determined in all three test conditions. In a separate set of experiment, LPV was incubated in enzyme free buffer for 30 min to determine absence of LPV degradation in buffer (data not shown).

Effect of excipients present in SLN formulation on metabolic function of the microsomal enzyme system was examined by incubating blank SLNs (SLNs prepared without drug) along with free LPV. Any difference in metabolism (compared with free LPV alone) was taken as enzyme inhibition.

Lopinavir uptake study into rat everted gut sac

Everted gut sac studies in rats were performed using established methods adapted from literature.[24] For the study, male Wistar rats were fasted overnight for 12 h and sacrificed by cervical dislocation. The rat intestinal segments were identified and separated from the body. A length of 8–10 cm from jejunum was rapidly removed and gently everted over a glass rod. Everted intestine was then slipped off the glass rod and placed in a flat dish containing KHB buffer oxygenated with O_2/CO_2 (95%/5%) at 37°C. Further, KHB solution (0.5 ml) was filled in to the everted gut sac. The sac was sealed by tying open ends with silk thread. Intestinal sacs were then placed in individual incubation chambers containing free LPV (2.5 µg/ml), LPV/RTV (LPV and RTV at an effective concentrations of 2.5 µg/ml and 0.625 µg/ml respectively) coformulation and LPV SLNs (2.5 µg/ml) prepared in KHB buffer at maintained temperature of 37°C.

In order to discern the uptake mechanism, permeability studies for LPV in free LPV, LPV/RTV coformulation and LPV loaded SLNs were conducted in the presence of specific endocytosis inhibitors; chlorpromazine (CPZ, 10 µg/ml) and nystatin (NYT, 25 µg/ml). After an incubation time of 60 min, intestinal sacs were carefully removed, blotted onto filter paper and contents were collected. Intestinal sacs were rinsed thrice with KHB solution and rinsings were pooled with original content for analysis. Samples were analyzed with a validated HPLC method.

P_{app} values, expressed in cm/s, were calculated in each experimental condition using the following Equation (3):

$$P_{app} = dQ/dt/A * C_o \tag{3}$$

where dQ/dt is the rate of appearance of LPV in the everted gut sac (receiver compartment), C_o is the initial concentration of LPV outside everted gut sac (donor compartment) and A is total cross sectional area of tissue.

HPLC analysis

Plasma samples were analyzed for determination of LPV using previously reported RP-HPLC method.[23] Briefly, Shimadzu LC-20 AD Series HPLC system (Shimadzu Corporation, Kyoto, Japan) consisting of Shimadzu LC-20 AD HPLC pump, Shimadzu series DGU-20A5 Degasser and a Shimadzu SIL HTC auto-sampler was used to inject 75 µl aliquots of the processed samples on an endcapped RP-C18 column (Luna, 250 × 4.6 mm, 5 µm, Phenomenex, Torrance, CA, USA), which was maintained at a temperature of 40°C. The isocratic mobile phase consisted of an aqueous phase (10 mM ammonium acetate, pH 6.5) and acetonitrile (35 : 65 v/v). LPV was monitored at a wavelength of 210 nm.

Analytical method was partially validated for analysis of LPV in tissue samples; spleen, mesenteric lymph node and liver. No interference was observed by tissue matrices at the retention time of LPV. Method was found to be reproducible with good recovery (over 90%) for the drug. A single-step protein precipitation technique was used to extract LPV from the rat plasma matrix and tissue samples. The detector response was linear over the concentration range of 200 ng/ml to 4000 ng/ml.

Statistical analysis

All in-vitro studies were performed in triplicate, and data from these experiments are expressed as mean ± standard deviation. Noncompartmental pharmacokinetic analysis was performed using Phoenix WinNonlin (Pharsight Inc., Mountain View, CA, USA) to determine various pharmacokinetic parameters. Unpaired *t*-test or analysis of variance (ANOVA), followed by Dunnett's test (Graphpad Prism, version 5.03, GraphPad Software, Inc., La Jolla, CA, USA) was used to assess any significance of difference between means. The significance level was set at 5%.

Results

Experimental design

Preliminary experiments

Critical process variables in preparation of SLN were screened using low resolution PBD. Particle size of SLN and EE of LPV were taken as critical quality attributes. From PBD, amount of lipid, surfactant type, surfactant concentration and ultrasonication time were found to be most critical variables influencing EE and particle size. For evaluation of the effect of surfactant type two surfactants, Tween 80 and PVA were selected. Formulations prepared with Tween 80 (1% w/v) showed low particle size (245.2 ± 2.2 nm) and moderate EE (40.4 ± 3.3%). However, formulations with PVA (1% w/v) showed particle size of 239.5 ± 3.2 nm and EE of 75.6 ± 2.1%. Difference in EE is explained by the difference in saturation solubility of LPV in aqueous solution of these surfactants. The saturation solubility of LPV in Tween 80 and PVA solutions (1% w/v) were 45.8 ± 1.4 µg/ml and 2.5 ± 0.8 µg/ml, respectively. Hence, PVA was selected as surfactant for further trials.

Box–Behnken design

Selected critical variables showed statistically significant influence on particle size and EE (Table 3). Quadratic equations establishing main effects and interaction effects were determined based on estimation of statistical parameters generated by Design Expert software. Statistical validation of quadratic equations was confirmed by ANOVA. In Figures 1a–d, response surface graphs illustrating the effects of critical variables on the particle size and the EE of SLN are presented.

Effects on particle size (Y_1)

As shown in Table 2, particle size of formulations ranged between 217 nm (run 16) and 415.0 nm (run 8); this indicated sensitivity of critical variables selected for study. Experiments carried out at centre points (run 1, 6, 13, 16 and 17; $n = 5$) of the design indicate reproducibility of experiment as coefficient of variation (CV) is less than 2%. Independent factors affecting particle size can be explained by following quadratic Equation (4):

$$Y_1 = 219.7 - 9.76(X_1) + 18.3(X_2) + 2.19(X_3) \\ + 0.75(X_1 X_2) + 3.53(X_1 X_3) - 29.90(X_2 X_3) \quad (4) \\ + 90.34(X_1^2) + 47.96(X_2^2) + 40.49(X_3^2)$$

A regression coefficient (r^2) of 0.9432 for the equation indicated a good correlation between observed response and selected critical variables. Residuals were distributed randomly around zero, and there was no effect of experimental sequence on the trend of residuals.

Effects on entrapment efficiency (Y_2)

As shown in Table 2, EE varied between 45.1% (run 11) to 83.0% (run 1), which indicates that the response was sensitive toward selected factors. Experiments performed at the centre points of the design (run 1, 6, 13, 16 and 17; $n = 5$) confirmed that the experimental method was highly reproducible (CV < 3%). From data presented in Table 3, it is evident that independent factors affecting EE were; concentration of surfactant (X_1), amount of lipid (X_2) and time of ultrasonication (X_3).

Effect can be explained by following second-order polynomial quadratic Equation (5):

Table 3 Statistical analysis results of particle size and entrapment efficiency (EE)

Source	Sum of Squares	DF	F-value	P-value	Sum of Squares	df	F-value	P-value
			Particle size (Y_1)				EE (Y_2)	
Model	68738.63	9	14.54	0.001[b]	2237.02	9	57.19	0.0001[b]
X_1	4145.05	1	7.89	0.0262[b]	176.72	1	40.66	0.0004[b]
X_2	2679.12	1	5.1	0.049[b]	1078.8	1	248.22	0.0001[b]
X_3	2363.28	1	4.5	0.0716[b]	71.4	1	16.43	0.0049[b]
$X_1 X_2$	2.25	1	0.0042	0.9497[b]	50.41	1	11.6	0.0114[b]
$X_1 X_3$	49.7	1	0.095	0.7674[b]	46.24	1	10.64	0.0138[b]
$X_2 X_3$	3576.04	1	6.81	0.035[b]	6.5	1	1.5	0.2608[b]
X_1^2	34361.53	1	65.41	0.0001[b]	232.91	1	53.59	0.0002[b]
X_2^2	9685.9	1	18.44	0.0036[b]	195.41	1	44.96	0.0003[b]
X_3^2	6902.05	1	13.14	0.0085[b]	294.45	1	67.75	0.0001[b]
Residual	3677.53	7			30.42	7		
Lack of fit	3661.73	3	309.01	0.078[b]	1.62	3	0.075	0.9702[b]
Pure error	15.8	4			28.8	4		
Total	72416.16	16			2267.44	16		

[a]Significant at $P < 0.05$. [b]Not significant at $P < 0.05$ (nonsignificant lack of fit).
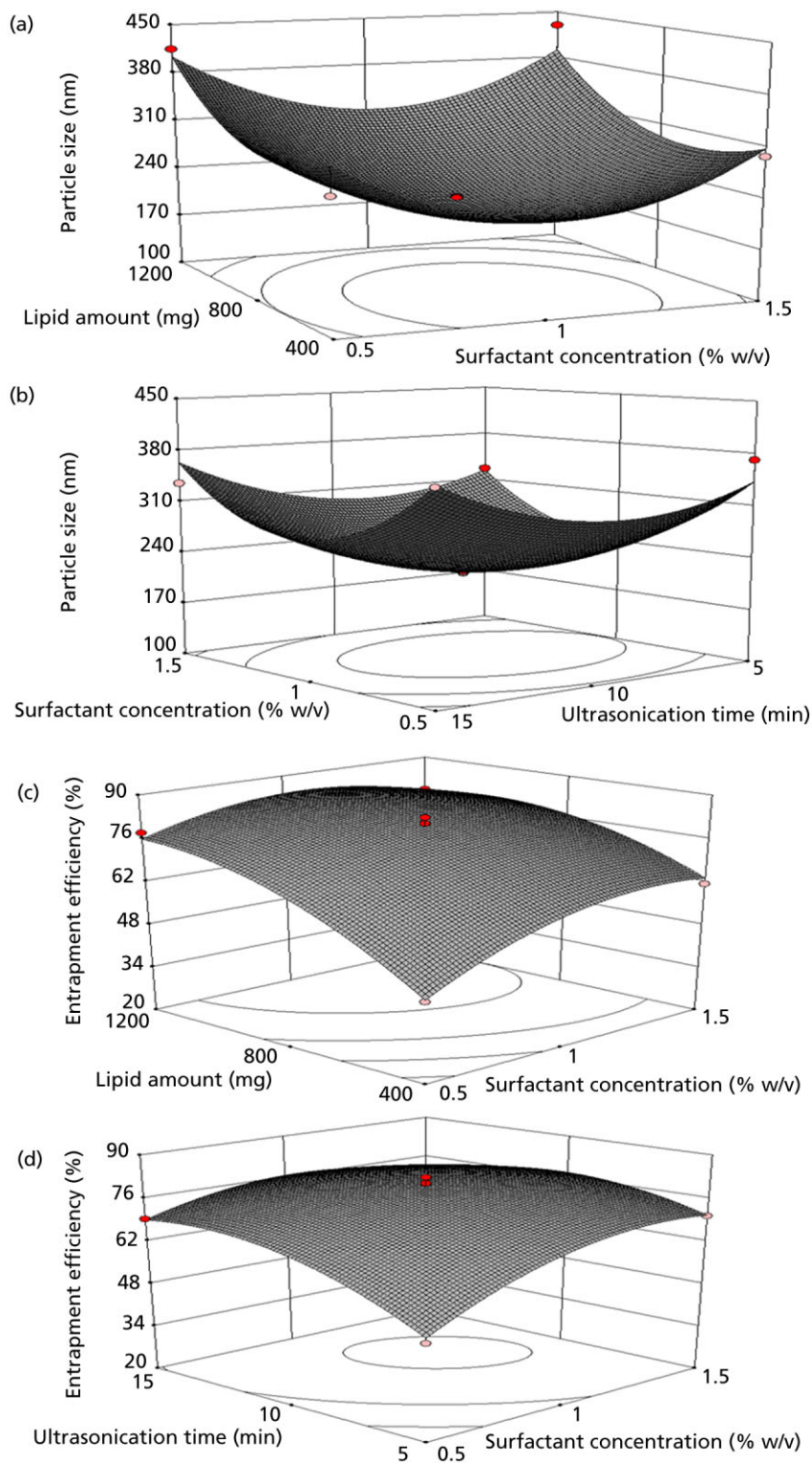
Figure 1 (a) Response surface plot showing the effect of surfactant concentration (X_1) and lipid amount (X_2) on particle size. (b) Response surface plot showing the effect of surfactant concentration (X_1) and ultrasonication time (X_3) on particle size. (c) Response surface plot showing the effect of surfactant concentration (X_1) and lipid amount (X_2) on entrapment efficiency. (d) Response surface plot showing the effect of surfactant concentration (X_1) and ultrasonication time (X_3) on entrapment efficiency.

$$Y_2 = 79.80 + 6.70(X_1) + 11.61(X_2) + 3.99(X_3)$$
$$- 3.55(X_1 X_2) - 3.40(X_1 X_3) - 1.27(X_2 X_3) \quad (5)$$
$$- 7.44(X_1^2) - 6.81(X_2^2) - 8.36(X_3^2)$$

Regression value of above equation was 0.9866 indicating suitability of the selected design model. Residual analysis showed that residuals were normally distributed around zero, and there was no trend of residuals on the outcome.

Optimization and validation

To acquire optimized formulation, desirability function (0.95) was probed using Design Expert software. As shown in Table 1, selection of optimum formulation was based on preset criteria. Conditions for optimal formulation as predicted by the software were as follows: surfactant concentra-

Figure 2 Scanning electron microscopic image of the optimized lopinavir solid lipid nanoparticles.

tion = 1.09% (w/v), lipid amount = 880.23 mg and duration of ultrasonication = 9.05 min. To prove the validity of this statistical model, verification runs ($n = 6$) with these conditions were carried out; Wilcoxon signed-rank test was used to identify statistically significant difference between actual and theoretical values. At $\alpha = 0.05$, there was no statistically significant difference between actual and theoretical values for particle size ($P \geq 0.0867$) and EE ($P \geq 0.875$). This affirms the validity of proposed model. Optimized formulation exhibited particle size of 223.3 ± 4.3 nm and EE of $83.1 \pm 2.35\%$.

Physicochemical characterization of lopinavir solid lipid nanoparticles

From SEM photomicrograph, near spherical shape of optimized LPV SLN was evident (Figure 2). Mean particle size, PDI (Figure 3) and zeta potential value of optimized LPV SLNs ($n = 6$) were 223.3 ± 4.3 nm, 0.21 ± 0.11 and -21.23 ± 2.5 mV, respectively. Negative zeta potential was attributed to the presence of free carboxylic acid groups in SA.

Figure 4 shows DSC thermograms for pure LPV, bulk SA (lipid), bulk PVA, physical mixture of LPV+SA (1 : 1), LPV+PVA (1 : 1), LPV+SA+PVA (1 : 1 : 1), blank SLNs and LPV SLNs. DSC thermogram for pure LPV showed sharp melting peak at 95.2°C, while bulk SA showed melting peak at 69.8°C. In DSC thermograms of blank and LPV SLNs, an additional peak observed at 168.3°C was of mannitol (used as cryoprotectant).

Figure 5 represent in-vitro drug release profiles of optimized SLNs and free LPV. Free LPV completely released from dialysis bag within 5 h. LPV SLNs showed a biphasic release pattern; this was characterized by an initial rapid release (45%) in the first 8 h followed by slow and continuous drug release up to 96 h. Drug release kinetics was
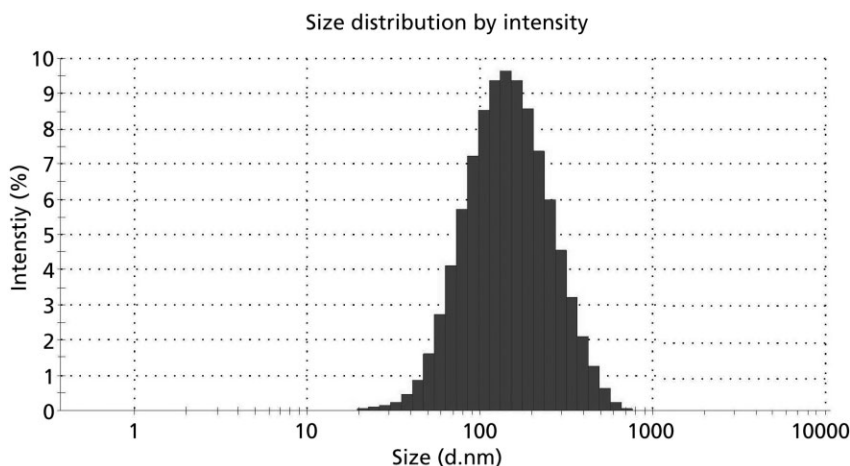
Figure 3 Particle size distribution of optimized lopinavir solid lipid nanoparticles.
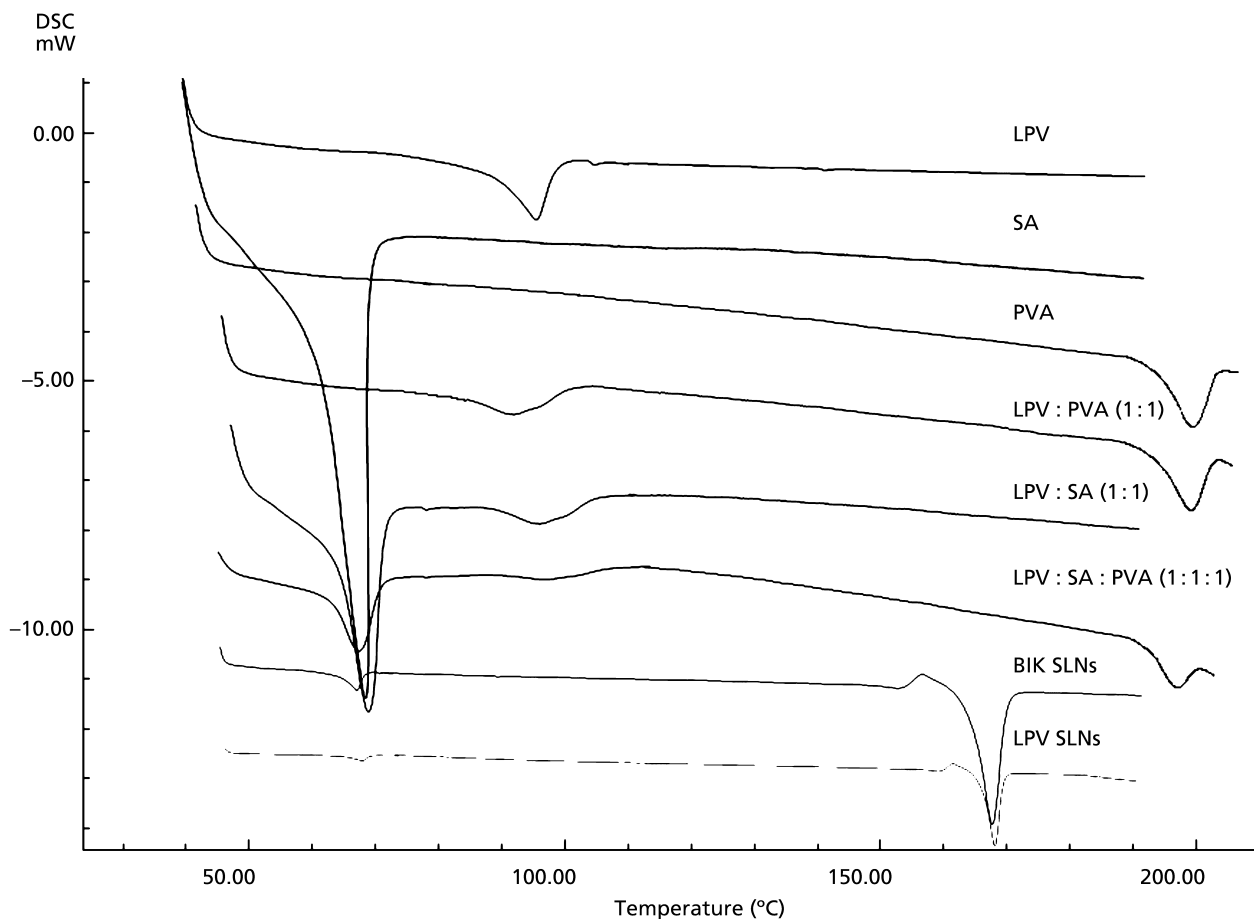
Figure 4 Overlaid differential scanning calorimetry thermograms of pure lopinavir, bulk stearic acid (lipid), bulk polyvinyl alcohol, physical mixture of lopinavir : polyvinyl alcohol (1 : 1), lopinavir : stearic acid (1 : 1), lopinavir : stearic acid : polyvinyl alcohol (1 : 1 : 1), blank solid lipid nanoparticles and lopinavir solid lipid nanoparticles.
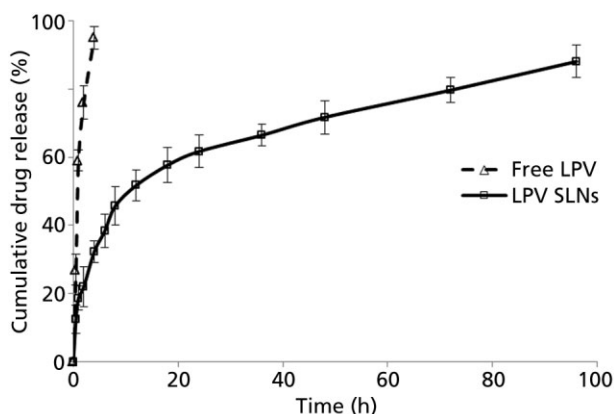
Figure 5 In-vitro drug release profile of free lopinavir and lopinavir solid lipid nanoparticles in phosphate buffer saline pH 7.4.

studied by fitting data into various mathematical models. From regression analysis, drug release from SLNs was most appropriately described by reciprocal-powered time model ($r^2 = 0.9763$). In comparison, zero-order kinetics ($r^2 = 0.3198$), first-order kinetics ($r^2 = 0.9437$) and Higuchi kinetics ($r^2 = 0.8784$) showed relatively lower r^2 values. Time taken for 50% drug release (t_{50}) from SLNs was calculated to be 11.21 h.

Stability studies

Stability estimation for optimized LPV SLN suspension was done on the basis of particle size, EE, zeta potential and PDI variations during 3-month study period. Results show that there was no significant ($P < 0.05$) change in assessed parameters when LPV SLNs are stored at 2–8°C. Similarly, SLN sample stored at $25 \pm 2°C/60 \pm 5\%$ RH showed no significant ($P < 0.05$) change in particle size and zeta potential. However, in these samples, statistically significant reduction in EE was observed. The EE of SLNs at the end of

3 months was 70% of initial formulation (data not shown). Hence, storage of SLN under refrigerated condition is recommended.

Pharmacokinetic studies

Comparative pharmacokinetic performances of free LPV, LPV/RTV coformulation and optimized LPV SLNs following oral administration to male Wistar rats are shown in Figure 6 and Table 4.

Following oral administration, both LPV/RTV coformulation and LPV SLNs showed statistically significant improvement in the pharmacokinetics of LPV as determined by area under the curve (AUC), maximum plasma concentration (C_{max}) and mean residence time (MRT).

Coadministration of RTV with LPV (Group B) significantly increased LPV AUC by 3.7 folds ($P < 0.001$), C_{max} by 2.1 folds ($P < 0.001$) and MRT by 1.5 folds ($P < 0.05$) as compared with free LPV (Group A). Whereas, LPV SLNs (Group C) increased LPV AUC by 5.1 folds ($P < 0.001$), C_{max} by 2.6 folds ($P < 0.001$) and MRT by 1.7 folds ($P < 0.05$).

Statically no significant effect was observed on time to reach the maximum plasma concentration (t_{max}) in either of the treatment groups as compared with free LPV.

Lopinavir uptake study into rat everted gut sac

Table 5 presents a comparison of apparent permeability (P_{app}) values of LPV after 60 min incubation through rat everted gut sacs. Experimental results demonstrated a significant increase in P_{app} values of LPV in LPV/RTV coformulation and LPV SLNs as compared with free LPV (control group). Coadministration of RTV with LPV significantly increased P_{app} of LPV by 2.7 folds ($P < 0.01$) as compared with control group. Whereas, the P_{app} of LPV SLNs was found to increase by 1.9 folds ($P < 0.01$) as compared with control group.

In order to investigate the mechanism of SLNs uptake into everted gut sac, intestinal uptake study of LPV was further performed in the presence of CPZ and NYT. Results revealed that the presence of specific inhibitors significantly ($P < 0.05$) reduced the intestinal permeability of SLNs. The
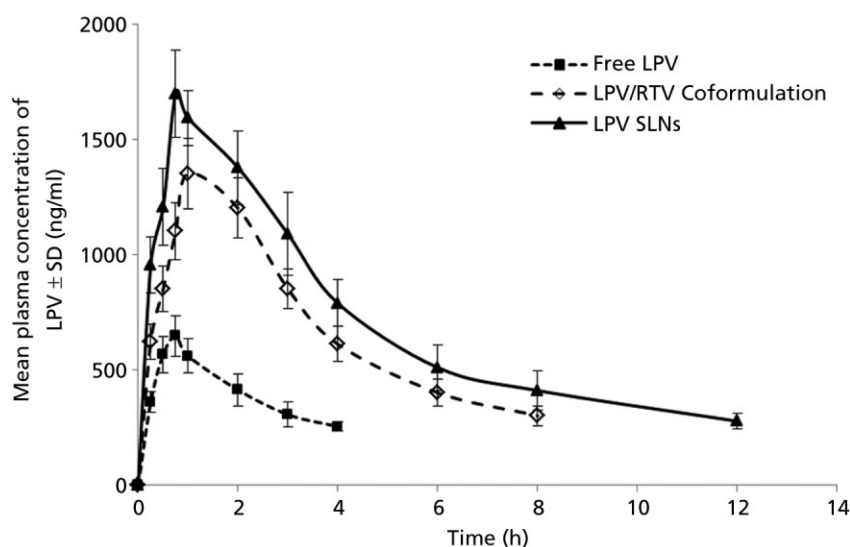
Figure 6 Mean plasma concentration-time profile of lopinavir following oral administration of free lopinavir, lopinavir/ritonavir coformulation and lopinavir solid lipid nanoparticles to Wistar rats ($n = 5$). The data are expressed as mean ± standard deviation.

Table 4 Pharmacokinetic parameteres of LPV following oral administration of free LPV, LPV/RTV coformulation and LPV SLNs to Wistar rats ($n = 5$)

Route	Parameters	Free LPV (Group A)	LPV/RTV (Group B)	LPV SLNs (Group C)
Oral (LPV, 20 mg/kg)	C_{max} (ng/ml)	645.85 ± 89.7	1350.45 ± 113.41[b]	1694.39 ± 156.59[b]
	T_{max} (h)	0.85 (0.75–1.0)	0.89 (0.75–1.0)	1.4 (0.75–2.0)
	MRT(h)	5.09 ± 0.25	7.81 ± 0.47[a,c]	8.57 ± 0.52[a]
	AUC (ng/ml[a]h)	1655.52 ± 53.34	6151.75 ± 112.45[b]	8402.05 ± 98.59[b]
	F_{rel}		3.72 ± 0.21	5.07 ± 0.35

[a]Statistically no significance difference ($P > 0.05$) between Group B and C; [b]Statistically significance difference ($P < 0.001$) as compared to Free LPV (Group A); [c]Statistically significance difference ($P < 0.05$) as compared to Free LPV (Group A). The data are expressed as mean ± S.D. LPV, lopinavir; RTV, ritonavir; SLNs, solid lipid nanoparticles.

Table 5 Effect of endocytic uptake inhibitors (chlorpromazine, 10 µg/ml and nystatin, 25 µg/ml) on intestinal permeability of free LPV, LPV/RTV coformulation and LPV SLNs

Groups	P_{app} ($\times 10^{-5}$ cm/s)		
	Control (without inhibitor)	(+) CPZ	(+) NYT
Free LPV	2.62 ± 0.31	2.85 ± 0.28	2.71 ± 0.29
LPV/RTV	$6.98 \pm 0.36^{a,b}$	7.21 ± 0.48^{b}	6.88 ± 0.41^{b}
LPV SLNs	5.18 ± 0.36^{a}	3.76 ± 0.21^{c}	3.22 ± 0.14^{c}

CPZ, chlorpromazine; LPV, lopinavir; NYT, nystatin; RTV, ritonavir; SLNs, solid lipid nanoparticles. [a]Statistically significance difference ($P < 0.01$) as compared with Free LPV; [b]Statistically no significance difference ($P > 0.05$); [c]Statistically significance difference ($P < 0.05$) as compared with LPV SLNs without inhibitor. The data are expressed as mean ± standard deviation

P_{app} of LPV SLNs was reduced by 27% than control after coincubation with CPZ. Similarly, in the presence of NYT, P_{app} of LPV SLNs significantly decreased by 38% than control. However, statistically no significant change in P_{app} values of LPV either in free LPV group or in LPV/RTV coformulation was observed in the presence of endocytic uptake inhibitors.

In-vitro metabolic stability study of lopinavir

Results obtained from in-vitro metabolic stability studies using RIMs and RLMs are shown in Figure 7. Mean percentage metabolism of LPV was reduced significantly ($P < 0.001$) upon coincubation with RTV (metabolism of 8.5% in RIMs; 7.8% in RLMs) as compared with free LPV (metabolism of 89.2% in RIMs; 81.3% in RLMs) after 30 min of incubation period in both of the microsomes. Similarly, mean percentage metabolism of LPV in LPV SLNs (metabolism of 14.1% in RIMs; 18.4% in RLMs) was found to significantly ($P < 0.001$) reduced as compared with free LPV. However, statistically no significant change in metabolism of free LPV was observed upon coincubation with blank SLNs.

Tissue distribution study

Tissue distribution study was done for free LPV, LPV/RTV coformulation and LPV SLNs to determine the exposure of LPV in target organs (liver, spleen and mesenteric lymph nodes).

As shown in Figure 8, statistically significant accumulation of LPV from LPV SLNs was observed in all three tissues of interest. In comparison with free drug, in liver tissue, C_{max} of LPV from SLN increased by 1.8 folds and AUC increased by 1.9 ($P < 0.01$). Similar observation was made in spleen tissue where C_{max} increased by 2.4 folds ($P < 0.001$), AUC increased by 2.3 folds ($P < 0.001$) for LPV SLN. In lymph nodes, accumulation of LPV from SLN was

evident. Here, for LPV SLN, C_{max} increased by 2.5 folds and AUC by 2.6 folds.

Following coadministration of LPV with RTV, statistically significant ($P < 0.05$) accumulation of LPV in liver tissue was observed. In this case, when coadministered with RTV, LPV's C_{max} increased by 1.3 folds and AUC increased by 1.4 folds. However, for spleen and lymph nodes, no statistically significant change in C_{max} and AUC was observed.

Discussion

Experimental design

Utility of statistical design in screening of variables and manufacture of SLN was reaffirmed from the results of experimental design. Figure 1a shows the effect of surfactant concentration and lipid amount on particle size at fixed ultrasonication time. It was observed that an increase in amount of lipid caused a corresponding increase in particle size. With increasing lipid amount in external phase, interfacial tension between lipid and aqueous phase increases leading to coalesce and increase in particle size.[25]

For a fixed amount of lipid, effect of surfactant concentration on particle size was nonlinear (Figure 1a). Increase in PVA concentration up to 1% w/v decreased particle size. Beyond this concentration, particle size increased. Initial reduction of particle size by PVA is due to reduction of interfacial tension between lipid and aqueous phase and stabilization of newly formed particles (due to steric stabilizing effect).[26] However, at higher concentrations, hydrophobic interactions between PVA molecules dominate, leading to aggregation and increase in particle size.

From Figure 1b, it is evident that the curvature of ultrasonication time is gradual. However, surfactant concentration shows significant curvature in the same figure. Hence, we infer that within selected limits, ultrasonication time does not influence particle size significantly.

Effect of surfactant concentration and lipid amount on the EE is shown in Table 3 and illustrated in Figure 1c. Steep curvature for EE when viewed from lipid axis indicates that with increasing amount of lipid, EE increases. With increase in lipid amount, LPV's entrapment in lipophilic matrix increases. Higher amount of lipid also provides additional number of particles into which LPV gets entrapped.

From Figure 1c, at fixed ultrasonication time, EE significantly increases by increasing both amount of surfactant and amount of lipid. This effect may be explained by increased viscosity of medium which prevents rapid diffusion of LPV into the bulk of medium increasing its EE.[27] With increasing surfactant concentration, it is also possible that LPV gets entrapped in surfactant layer covering SLN surface leading to higher EE.

From Figure 1d, it is evident that ultrasonication time has a positive effect on EE. As time of ultrasonication
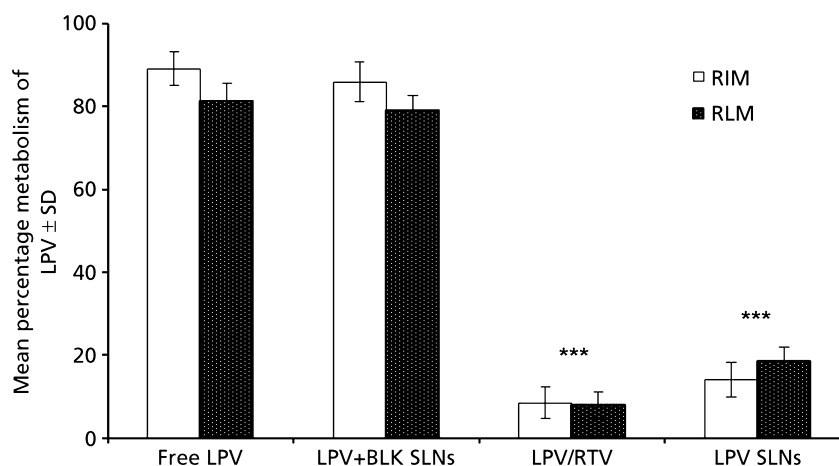
Figure 7 Metabolic stability of free lopinavir, lopinavir/ritonavir coformulation and lopinavir solid lipid nanoparticles after 30 min incubation with rat intestinal microsomes and rat liver microsomes at 1 mg/ml protein concentration. ***Statistically significance difference ($P < 0.001$) as compared with free lopinavir. The data are expressed as mean ± standard deviation.

increases, there is relative but insignificant ($P < 0.05$) reduction in particle size. This increases the surface area available for drug accommodation. The overall effect is increase in EE with increase in ultrasonication time.

Physicochemical characterization of solid lipid nanoparticles

Optimized formulation exhibited particles in nanometric size with high EE and low PDI value (Figure 3). Low PDI (below 0.2) indicates that optimal conditions are suitable for the production of stable LPV NPs with narrow size distribution.

In SLNs manufactured by hot melt emulsion technique, majority of incorporated drug remains in the core of lipid matrix.[26] However, a portion of the drug remains bound at lipid-surfactant interface. This disparity in drug distribution can result in biphasic drug release pattern from SLN. As evident from Figure 5, LPV-loaded SLN presented similar biphasic drug release pattern; initial burst release due to surface presence of LPV followed by more sustained release due to drug embedded in core of lipid matrix.

Various methods are available to assess the drug release from nanoparticulate systems. Use of dialysis bag in release studies is widely reported technique and convenient to perform.[28] However, it suffers from certain drawbacks. It has been reported that slow equilibration of drug with outer media limits an accurate analysis of initial drug levels in formulations where the burst release is high.[29] Therefore, in such cases true drug release profile could be under estimated.

In Figure 4, peak position of LPV in all the physical mixtures was found to be unaffected indicating absence of incompatibility between LPV and SA/PVA.

Ex vivo and in-vivo studies

Series of comparative pharmacokinetic studies were conducted to understand the mechanism involved in the pharmacokinetic improvement of LPV in LPV/RTV coformulation and LPV SLNs. Dose equivalent to LPV 20 mg/kg and RTV 5 mg/kg in LPV/RTV coformulation (Lopimune Tablets, Cipla Ltd) was selected based on Kaletra (Abbott Laboratories, LPV/RTV, 4 : 1) that is internationally marketed for treatment of HIV patients.

From oral pharmacokinetic studies, it is evident that LPV has poor bioavailability because of both high first-pass metabolism and P-gp efflux. Significant improvement in plasma exposure of LPV in the presence of RTV (coformulation) could be attributed to reduced first-pass metabolism and/or P-gp efflux. For the same reason, RTV is being marketed as a pharmacokinetic booster for LPV.

From our study, LPV SLNs demonstrated significant increase in plasma exposure compared to free LPV (Figure 6). High LPV exposure could be due to reduced first-pass metabolism and P-gp efflux. Additionally, uptake of LPV SLNs by lymphatic route also helps in bypassing first-pass metabolism and P-gp efflux thus increasing bioavailability of LPV.

Rat everted gut sac model was used to investigate intestinal permeability and uptake mechanism of LPV loaded SLNs. From the study, significant increase in P_{app} of free LPV in the presence of RTV was obtained. Therefore, it was evident that P-gp has a considerable role in limiting free LPV's bioavailability. However, in this study we have not considered the use of control inhibitors of cytochrome P450; attributing the outcome of study to P-gp modulation alone may not be accurate. In the present model,
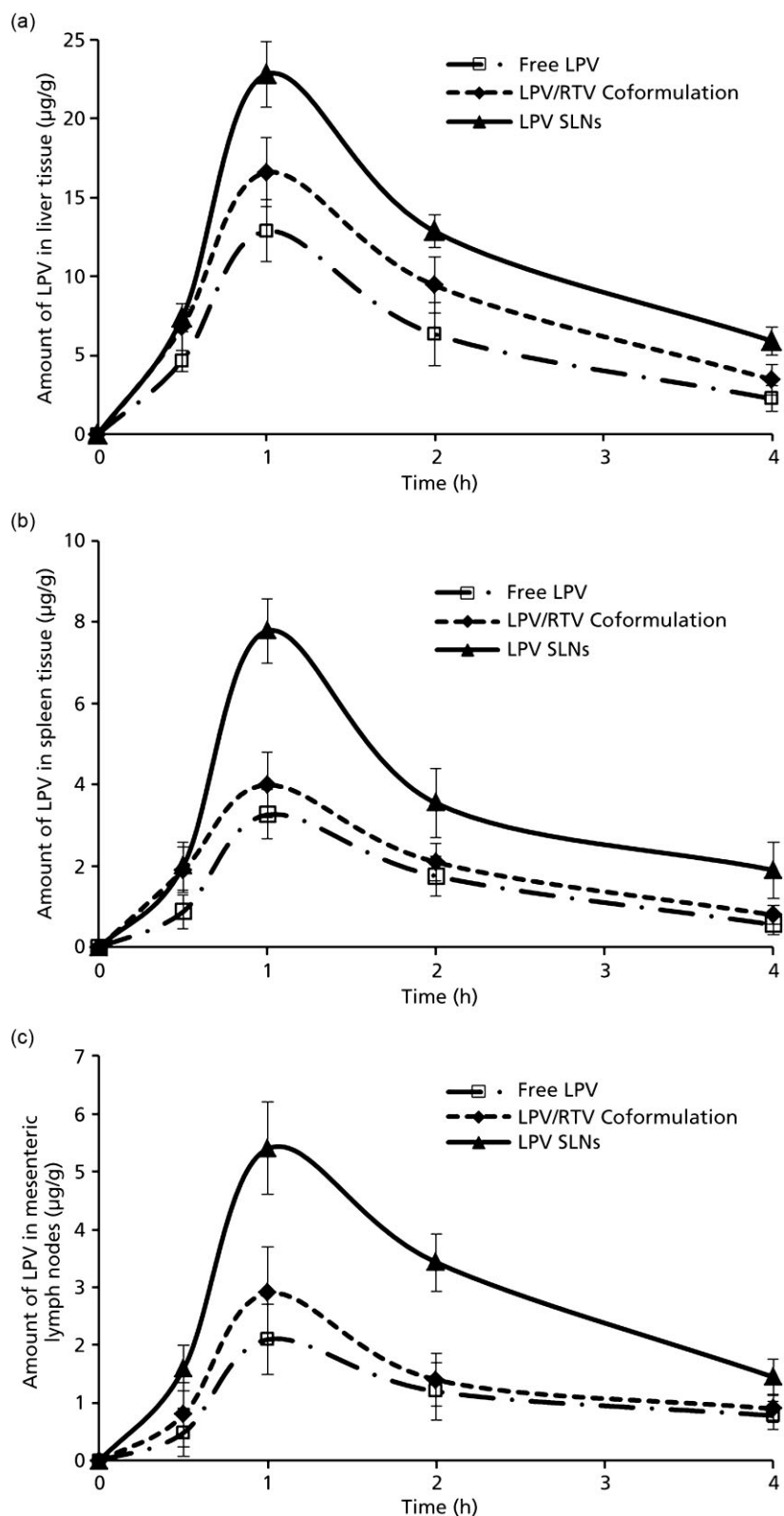
Figure 8 Tissue distribution study of free lopinavir and lopinavir/ritonavir coformulation and lopinavir-loaded solid lipid nanoparticles following oral administration to Wistar rats. Three animals were sacrificed at each time point to harvest (a) liver, (b) spleen and (c) mesenteric lymph node tissues. The data are expressed as mean ± standard deviation.

we could not distinguish the role of transporter from metabolism.

As compared with free LPV, significant increase in P_{app} for LPV SLNs suggests that SLNs could efficiently cross intestinal barriers while protecting the drug from P-gp efflux and CYP enzyme systems.

To establish uptake mechanism, studies were carried out with specific endocytosis (phagocytosis/pinocytosis) process inhibitors. CPZ and NYT were selected as uptake inhibitors because of their ability to inhibit clathrin coated pit associated receptors and abolishing caveolae function respectively.[30] Results from this study demonstrated a significant reduction in P_{app} of LPV SLNs in the presence of specific endocytic uptake inhibitors. This indicates that uptake of LPV SLNs occurs by endocytosis (phagocytosis) process. Further, it could be deduced that both clathrin and caveolae-mediated endocytosis mechanisms were involved in the uptake of LPV SLNs. Similar studies were also performed with free LPV and LPV/RTV coformulation using CPZ and NYT as uptake inhibitors. From P_{app} values presented in Table 5, it is evident that uptake of either free LPV or LPV/RTV coformulation was unaffected by the presence of uptake inhibitors. From this, we concluded that endocytosis plays an insignificant role in the uptake of LPV.

Results from metabolic stability study shows extensive metabolism of free LPV in presence of RLMs/RIMs. It was also evident that SLNs could offer metabolic protection to LPV, which is akin to RTV. Drastic increase in plasma levels of LPV after coadministration with RTV is due to inhibition of CYP 3A enzyme system by RTV. Similarly, metabolic protection offered by SLNs to LPV (gut wall and liver) aids in achieving longer circulation time leading to higher plasma exposure.

Data obtained from tissue distribution studies indicate high localization of LPV in liver tissue as compared with spleen and lymph nodes. Superior blood perfusion to liver compared to other organs may result in accumulation of free LPV in liver. In case of loaded SLNs, higher distribution was seen in spleen and lymph nodes. This indicates lymphatic uptake of SLNs following oral administration. It has been reported that lipid nanoparticles reach lymphatic system either by direct endocytosis/transcytosis uptake by membranous epithelial cells (M-cells) covering Payer's patches in intestine or by conversion into triglyceride-rich lipoprotein particles called chylomicrons, which are secreted into intestinal lymph.[31] Metabolic protection offered to LPV by RTV leads to higher accumulation of LPV in liver tissue. This augments with the results from in-vitro metabolic stability data. However, it is noteworthy that RTV coadministration failed to increase LPV concentration in poorly perfused organs like spleen and lymph nodes, while, LPV-loaded SLNs produced significantly higher levels in these organs.

It is reported that viral reservoirs present in lymphoidal organs are poorly accessed by conventional therapy. In conventional therapy, minimum effective concentration of drug can not be maintained for the necessary time duration at the site of HIV localization.[9] Higher distribution of LPV SLNs in such tissues at all time points assures higher LPV availability in these reservoirs. Thus, as compared to conventional LPV/RTV therapy, better therapeutic outcome of LPV from LPV SLN could be expected.

Conclusions

LPV was successfully loaded in SLNs with high EE and desirable particle size range. Processing conditions for the manufacture of these LPV SLNs were identified and optimized using DoE with good correlation between actual and predicted values. Plasma exposure of LPV from LPV SLNs was comparable with exposure obtained from LPV/RTV coformulation.

Metabolic protection and increased intestinal permeability were demonstrated as possible reasons for improving LPV oral bioavailability in either of the formulations. Relatively higher distribution of LPV SLNs in poorly perfused lymphoidal tissues as compared to LPV/RTV coadministration suggests that LPV loaded SLNs could be safer and more effective alternative to currently marketed LPV/RTV coformulation.

In conclusion, formulating SLNs for poorly soluble LPV was an effective approach in improving its oral bioavailability and LPV exposure to HIV reservoirs, which may prove beneficial in the treatment of HIV-infected patients.

Declarations

Conflict of interest

The authors declare that they have no conflicts of interest to disclose.

Funding

References

1. Freed EO. HIV-1 Replication. *Somat Cell Mol Genet* 2001; 26: 13–33.

2. Schrager LK, D'Souza MP. Cellular and anatomical reservoirs of HIV-1 in patients receiving potent antiretroviral combination therapy. *JAMA* 1998; 280: 67–71.

3. Pomerantz RJ. Reservoirs of human immunodeficiency virus type 1: the main obstacles to viral eradication. *Clin Infect Dis* 2002; 34: 91–97.

4. Pierson T *et al.* Reservoirs for HIV-1: mechanisms for viral persistence in the presence of antiviral immune responses and antireteroviral therapy. *Annu Rev Immunol* 2000; 18: 665–708.

5. Sharma A *et al.* Recent Advances in NDDS (Novel drug delivery systems) for delivery of Anti- HIV drugs. *Res J Pharm Bio Chem Sci* 2010; 1: 78–88.

6. Farmer P *et al.* Community-based treatment of advanced HIV disease: introducing DOT-HAART (directly observed therapy with highly active antiretroviral therapy). *Bull World Health Organ* 2001; 79: 1145–1151.

7. Temesgen Z *et al.* Current status of antiretroviral therapy. *Expert Opin Pharmacother* 2006; 7: 1541–1554.

8. du Plooy M *et al.* Evidence for time dependent interactions between ritonavir and lopinavir/ritonavir plasma levels following P-glycoprotein inhibition in Sprague-Dawley rats. *Biol Pharm Bull* 2011; 34: 66–70.

9. Wong HL *et al.* Nanotechnology applications for improved delivery of antiretroviral drugs to the brain. *Adv Drug Del Rev* 2010; 62: 503–515.

10. Kaletra Tablets and Oral Solutions, 2013. Accessed on 22 January 2014. Available from: http://www.medsafe.govt.nz/profs/datasheet/k/Kaletratabsoln.pdf

11. Piacenti FJ. An update and review of antiretroviral therapy. *Pharmacotherapy* 2006; 26: 1111–1133.

12. Shafran SD *et al.* The effect of low dose ritonavir monotherapy on fasting serum lipid concentrations. *HIV Med* 2005; 6: 421–425.

13. Cai S *et al.* Lymphatic drug delivery using engineered liposomes and solid lipid nanoparticles. *Adv Drug Deliv Rev* 2011; 63: 901–908.

14. Kingsley JD *et al.* Nanotechnology: a focus on nanoparticles as a drug delivery system. *J Neuroimmun Pharmacol* 2006; 1: 340–350.

15. Aji AMR *et al.* Lopinavir loaded solid lipid nanoparticles (SLN) for intestinal lymphatic targeting. *Eur J Pharm Sci* 2011; 42: 11–18.

16. Negi JS *et al.* Development of solid lipid nanoparticles (SLNs) of lopinavir using hot self nanoemulsification (SNE) technique. *Eur J Pharm Sci* 2013; 48: 231–239.

17. Xu X *et al.* A quality by design (QbD) case study on liposomes containing hydrophilic API: I. Formulation, processing design and risk assessment. *Int J Pharm* 2011; 419: 52–59.

18. Zhang Q *et al.* Studies on the cyclosporine a loaded stearic acid nanoparticles. *Int J Pharm* 2000; 200: 153–159.

19. Castelli F *et al.* Characterization of indomethacin-loaded lipid nanoparticles by differential scanning calorimetry. *Int J Pharm* 2005; 304: 231–238.

20. Yue PF *et al.* The study on the entrapment efficiency and i*n vitro* release of Puerarin submicron emulsion. *AAPS PharmSciTech* 2009; 10: 376–383.

21. Shah M, Pathak K. Development and statistical optimization of solid lipid nanoparticles of simvastatin by using 2^3 Full-Factorial Design. *AAPS PharmSciTech* 2010; 11: 489–496.

22. ICH Topic Q 1 A (R2). Stability Testing of new Drug Substances and Products. (CPMP/ICH/2736/99). 2003 Accessed on 22 January 2014, Available from: http://www.ema.europa.eu/docs/en_GB/document_library/Scientific_guideline/2009/09/WC500002651.pdf

23. Vats R *et al.* Simple, rapid and validated LC determination of lopinavir in rat plasma and its application in pharmacokinetic studies. *Sci Pharm* 2011; 79: 849–863.

24. Ravi PR *et al.* Effect of ciprofloxacin and grapefruit juice on oral pharmacokinetics of riluzole in Wistar rats. *J Pharm Pharmacol* 2013; 65: 337–344.

25. Leroux J *et al.* New approach for the preparation of nanoparticles by an emulsification-diffusion method. *Eur J Pharm Biopharm* 1994; 41: 14–18.

26. Hao J *et al.* Development and optimization of solid lipid nanoparticle formulation for ophthalmic delivery of chloramphenicol using a Box-Behnken design. *Int J Nanomedicine* 2011; 6: 683–692.

27. Yang Y *et al.* Effect of preparation conditions on morphology and release profiles of biodegradable polymeric microspheres containing protein fabricated by double-emulsion method. *Chem Eng Sci* 2000; 55: 2223–2236.

28. Kadajji VG *et al.* Approaches for dissolution testing of novel drug delivery systems. American Pharmaceutical Review. The Review of American Pharmaceutical Business and Technology. 2011 Accessed on 22 January 2014, Available from: http://www.americanpharmaceuticalreview.com/Featyred-Articls/36880-Approaches-for-Dissolution-Testing-of-Novel-Drug-Delivery-Systems/

29. D'Souza SS, DeLuca PP. Development of a dialysis in vitro release method for biodegradable microspheres. *AAPS PharmSciTech* 2005; 6: E323–E328.

30. Roger E *et al.* Lipid nanocarriers improve paclitaxel transport throughout human intestinal epithelial cells by using vesicle-mediated transcytosis. *J Cont Rel* 2009; 140: 174–181.

31. Porter C *et al.* Lipids and lipid based formulations: optimizing the oral delivery of lipophilic drugs. *Nat Rev Drug Discov* 2007; 6: 231–248.